Talanta 77 (2009) 1632–1639

Contents lists available at ScienceDirect

Talanta

journal homepage: www.elsevier.com/locate/talanta

Improved design for high resolution electrospray ionization ion mobility spectrometry

M.T. Jafari*

Department of Chemistry, Isfahan University of Technology, Isfahan 84156-83111, Iran

ARTICLE INFO

Article history:
Received 3 August 2008
Received in revised form
17 September 2008
Accepted 29 September 2008
Available online 17 October 2008

Keywords:
High resolution
Electrospray ionization
Ion mobility spectrometry

ABSTRACT

An improved design for high resolution electrospray ionization ion mobility spectrometry (ESI-IMS) was developed by making some salient modifications to the IMS cell and its performance was investigated. To enhance desolvation of electrospray droplets at high sample flow rates in this new design, volume of the desolvation region was decreased by reducing its diameter and the entrance position of the desolvation gas was shifted to the end of the desolvation region (near the ion gate). In addition, the ESI source (both needle and counter electrode) was positioned outside of the heating oven of the IMS. This modification made it possible to use the instrument at higher temperatures, and preventing needle clogging in the electrospray process. The ion mobility spectra of different chemical compounds were obtained. The resolving power and resolution of the instrument were increased by about 15–30% relative to previous design. In this work, the baseline separation of the two adjacent ion peaks of morphine and those of codeine was achieved for the first time with resolutions of 1.5 and 1.3, respectively. These four ion peaks were well separated from each other using carbon dioxide (CO_2) rather than nitrogen as the drift gas. Finally, the analytical parameters obtained for ethion, metalaxyl, and tributylamine indicated the high performance of the instrument for quantitative analysis.

1. Introduction

Ion mobility spectrometry (IMS) was developed for detection and characterization of chemical compounds such as illicit drugs, explosives, pharmaceuticals, environmental pollutants [1]. This technique has been recently used in high-throughput proteomics studies [2–4]. IMS technique can distinguish between compounds on the basis of differences in their reduced mass, charge, and collisional cross section under a weak electric field. Therefore, IMS enables resolution of closely related ionic species. It has also shown to be a valuable structural tool for determining gas-phase ion conformations [5,6].

Ionization source is one important part of an ion mobility spectrometer which produces ions at ambient pressure. Electrospray ionization (ESI), as an ionization source for IMS, converts sample molecules from liquid to gas phase ions. This nonradioactive ionization source has become attractive as a method for IMS determination of biomolecules [7–9]. This method may also be used for detection of inorganic compounds such as uranyl acetate in water [10]. The main advantages of ESI are possibility of direct introduction of liquid samples into IMS, retaining of molecular weight information due to the soft ionization processes, and formation of multiply charged ions in some instances [1]. A lot of liquid-phase separation techniques have been developed using mass spectrometry (MS) as detector. However, using a mass spectrometer as a detection system in separation techniques has some important problems such as complexity of the instrument and high price. In contrast, IMS has less complex instrumentation, high throughput, ease of operation, and low cost as a detector for liquid chromatography [11,12]. Hence, application of ESI-IMS was demonstrated as a detection method for liquid chromatography [13–16], capillary electrophoresis [17], and flow injection analysis [18]. The main limitation of ESI-IMS is, however, its low resolution which can be attributed to several points. First, a relatively large volume of sample is typically introduced for trace analysis. Solvent evaporation from the electrosprayed fine droplets in the drift region can, therefore, cause broadening of the analyte bands [19,20]. Second, heat transfer from the atmospheric gas to the sprayed droplets is low, and desolvation cannot be completed effectively before the droplets enter the drift region. Third, the electrical potential of the ESI source perturbs the homogeneity of the electric field in the drift region [21,22].

Electrospray ionization was first introduced as an ionization source for IMS in 1972 by Dole and co-workers [23]. They concluded that due to inefficient desolvation of the electrosprayed droplets, ESI would not find the same applicability in IMS as it does in MS, in

* Tel.: +98 311 391 2351; fax: +98 311 391 2350.
E-mail address: jafari@cc.iut.ac.ir.

0039-9140/$ – see front matter © 2008 Elsevier B.V. All rights reserved.
doi:10.1016/j.talanta.2008.09.059

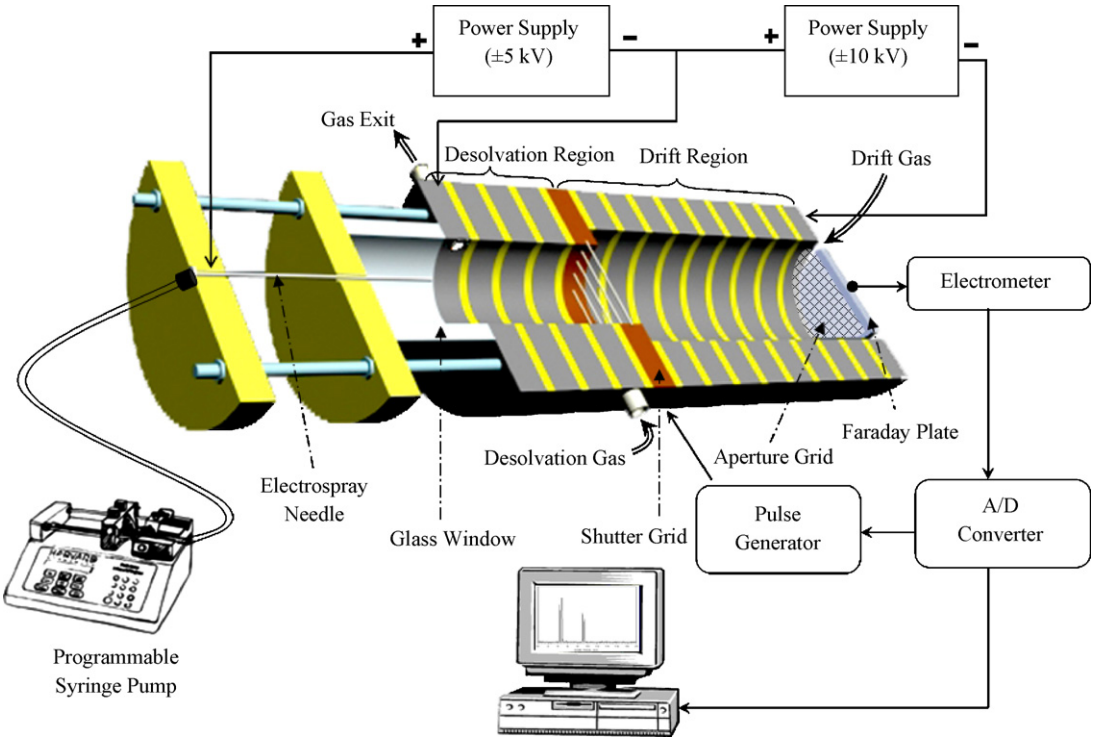

Fig. 1. The schematic diagram of the electrospray ionization-ion mobility spectrometer apparatus with improved design. The diameter of desolvation region was decreased to about half of the drift region diameter and the desolvation gas was entered into the cell at the end of the desolvation region.

which solvent can be readily evaporated under vacuum condition. Later, instrumental improvements such as adding a counterflow of a dry gas and a water-cooled electrospray ion source, suggested by Hill and co-workers, enhanced the desolvation efficiency and prevented needle clogging [19,24–27]. According to the equation derived by Siems et al. [22] for calculation of ion pulse duration measured at half of maximal intensity, lowering the drift tube temperature is an effective way to increase the resolving power of an ion mobility spectrometer. On the other hand, higher temperature of the countercurrent drift gas is necessary for efficient desolvation of the analyte ions.

In addition to the drift gas we recently [28] constructed an ESI-IMS with a preheated dry gas named "Desolvation Gas". Flowing the desolvation gas through the desolvation region of the IMS cell increased solvent evaporation and resulted in decreasing the drift time and increasing the resolving power. In that design, the electrospray needle was located outside of the cell oven. The consequence was to prevent prespray solvent evaporation problems inside the needle and therefore, needle clogging did not occur during the operation up to 130 °C.

Following these instrumental studies, this paper demonstrates further improvements in the design. In this new design, more efficient desolvation could be achieved by reducing the volume of the desolvation chamber in addition to proper entrance for desolvation gas. These modifications in the proposed design enable the use of higher flow rates at elevated temperature, preventing problems in the electrospray process.

2. Experimental

2.1. Ion mobility spectrometer

The electrospray ionization ion mobility spectrometer used in this research was designed and constructed at Isfahan University of Technology, Isfahan. The schematic diagram of the spectrometer is shown in Fig. 1. The key components of the system included the IMS cell, power supply and pulse generator devices, and signal processing program. The ESI-IMS cell was divided into three different sections named ESI source region, desolvation region, and drift region. This cell was constructed out of our previous design [28], but a number of modifications were made to further increase the operation performance of the instrument. These modifications included: (a) decreasing the volume of the desolvation region by reducing the inside diameter of this region, (b) moving the entrance position of the desolvation gas to the end of the desolvation region, and (c) locating the ESI source (including needle and counter electrode) completely outside of the heating oven.

In this work, the glass cell of the system was substituted with aluminum rings (as conducting rings), which were separated from each other by thin PTFE rings (as insulating rings) of 2 mm thickness. The drift and desolvation conducting rings have the dimensions of 60 mm (o.d.) × 40 mm (i.d.) × 10 mm (width), and 60 mm (o.d.) × 21 mm (i.d.) × 10 mm (width), respectively. The lengths of the drift and desolvation regions are 11 and 5 cm, respectively, but they can be easily shortened or lengthened by removing or adding a number of rings. Electrical contact between conducting rings of drift and desolvation regions was accomplished by using a series of 5.6 MΩ resistors. This configuration provided a uniform electric field inside the drift tube. A high voltage power supply (±10 kV, non-isolated) provided adequate voltage through a voltage divider for the entrance and exit of the desolvation and drift regions. An oven with a sufficient volume (22 L, 12 Bahman Co., Iran) was used to warm up the IMS cell as well as the drift and desolvation gases before entering the cell. The temperature of the heating oven can be chosen from 25 to 200 °C (±0.01). Pure nitrogen was employed as the drift and the desolvation gases with flow rates of 500 and 900 mL min^{-1}, respectively [28]. In order to remove water vapor or other contaminations, the gas was filtered with a 13× molecular sieves (Fluka) trap before entering the IMS cell. As shown in Fig. 1, the entrance tube of the desolvation gas

Table 1
Typical operating conditions during the experimental runs.

Operating parameters	Setting
Needle voltage (kV)	11.40
Target electrode voltage (kV)	9.00
Liquid flow rate (μL min^{-1})	10
Drift field (V cm^{-1})	600
Desolvation field (V cm^{-1})	600
Drift gas flow (N_2) (mL min^{-1})	500
Desolvation gas flow (N_2) (mL min^{-1})	900
Drift tube length (cm)	11
Shutter grid pulse (ms)	0.3
Number of IMS averages	50
Scan time (ms)	20
Number of points per ion mobility spectrum	500

was oriented ∼45° with respect to the drift tube axis to achieve the same direction as that of the drift gas. This figure also shows that the exhaust tube of the IMS cell is located on the first ring of the desolvation region (target electrode) to exit the warm gas before it reaches the needle tip.

Ion gating was achieved with a Bradbury–Nielsen gate [29] ring (21 mm i.d.) located at the end of the desolvation tube and the entrance of the drift tube. The Bradbury–Nielsen gate was made of electrically isolated alternating parallel alloy 26 wires (50 μm in diameter) with 0.75 mm spacing. The ion gate timing was set manually using a custom-built pulsing electronic device. The logic signals required by the pulsing electronics were generated through a personal computer equipped with an arbitrary waveform generator board. When the potentials applied on the alternating wires were the same as the reference potential, the gate was "open" to allow ions to pass through, whereas when the potentials on the adjacent wires were offset (85 V with respect to the reference potential) an electric field (∼2200 V cm^{-1}) was created orthogonal to the drift field of the spectrometer, and the gate was "closed" to shut off ion transmission. An aperture grid ring, made of an electrical joint between the last drift ring and a wire screen (stainless steel), was located at the end of the drift tube. The function of the aperture grid was to shield the incoming ion cloud from the detector prior to its arrival and hence reduce peak broadening.

The default Faraday plate detector configuration consisted of a stainless steel Plate 21 mm in diameter, positioned ∼1.0 mm behind the aperture grid. The Faraday plate detector was connected to a home-made current to voltage (A/V) amplifier with a gain of 10^9 V/A. The signal can be amplified, up to 1000 times, using a tunable-gain amplifier. The high-speed A/D module (12-bit dynamic range) was used to measure the spectrometer output and to convert the analog signal to a digital one. All mobility data were collected by data acquisition software and each IMS spectrum was the average of 50 individual spectra. Table 1 summarizes the operating conditions under which the IMS spectra were taken.

2.2. ESI ionization source

In this design, the ESI ionization region, comprising the electrospray needle and counter electrode was located completely outside the heating oven. A small glass-tube (15 cm length and 21 mm i.d.) was used as a window for observing the needle tip by illuminating it with a small diode laser. The glass window was sealed with the aluminum target electrode. A cap for the glass-tube was fabricated by machining a PTFE piece (40-mm o.d. × 10-mm thick) with a central hole 0.8 mm in diameter. This metal-glass-Teflon seal outside the oven serves as a joint for the varying temperature between the desolvation and ionization regions of the instrument. This modification allowed us to use the instrument without the need for a cooling system for the ESI needle, even at 200 °C. This temperature is the limit of our heating oven. In addition, the glass window allows the operator to observe the needle tip and to optimize the experimental conditions for producing a plume formation and a stable electrospray. A commercially available 26s-gauge polished needle (P/N 7768-01, Hamilton, Reno, NV, U.S.A.) with 0.13 mm i.d., 0.46 mm o.d., and a length of approximately 51 mm was used as the electrospray needle. The position of the ESI needle was adjusted such that its tip was located about 7 mm from the target electrode. A relatively large tip aperture was chosen in this research because it allowed liquid to be delivered through the emitter at a relatively wide range of flow rates. Normally, the flow rate varied from 1 to 40 μL min^{-1}. The solution was delivered from the same syringe (1.0 mL Hamilton gastight syringe, Reno, NV, U.S.A.) for the entire set of the experiments, to ensure consistency throughout. Sample solution was delivered to the electrospray ion source by a programmable syringe pump (New Era Pump System Inc., U.S.A.). A second high-voltage power supply (±5 kV, isolated) provided independent voltage control for the ESI ion source up to 15 kV. The electrical contact was applied through a stainless steel zerodead-volume union that connected the emitter with the PTFE capillary transfer line (2.0-mm o.d. × 0.2-mm i.d., ∼15 cm long). The corona discharge problem was eliminated by insulating the spray needle with a Teflon tubing [26,28]. The high-voltage power supply and pulse generator devices were prepared from Radyabchem. Co., Isfahan Science & Technology Town. Although the mixture of methanol, water, and acetic acid are commonly used for ESI-IMS, in this work, for better comparison of the results with those of the old instrument, pure methanol was used as the electrospray solvent. Electrospray ionization was normally induced by applying a potential difference of 2.0–3.0 kV between the electrospray needle and the target electrode, which also served as the first ring electrode for the desolvation region. In this work, an electrospray voltage of 11.4 kV (2.4 kV versus the desolvation chamber entrance) was used, and the electrospray flow rate was maintained at 10 μL min^{-1} for all experiments unless otherwise mentioned.

2.3. Chemicals and solutions

Methanol used as the electrospray solvent was high performance liquid chromatography (HPLC) grade and was purchased from Merck (Germany). The drug standards of morphine sulfate and codeine phosphate were prepared from Temad Co. (Tehran), and the methadone with concentration of 5 mg mL^{-1} was purchased from Darou pakhsh Co. (Tehran). Pesticides including ethion, Malathion, fenamifos, and metalaxyl were prepared from Accustandard, Inc. (U.S.A.). All the amines and furfurals used in this work were purchased from Merck. Unless specified, samples were prepared at a concentration of 1.0 mg L^{-1} for obtaining the IMS spectra. Stock standard solutions of 100 μg mL^{-1} ethion, metalaxyl, and tributylamine were prepared in methanol. Working solutions (0.01–20 μg mL^{-1}) were prepared by successive dilution of the stock solutions.

3. Results and discussion

3.1. Desolvation efficiency

To investigate the extent of desolvation process with the proposed design, ESI-IMS spectra of some chemicals such as drugs, pesticides, and some amines and furfurals were obtained and the reduced mobility values (K_0) of produced ions were calculated. Comparison of K_0 values obtained through electrospray ionization and the conventional ^{63}Ni can be used as an extent of the desolvation efficiency of sprayed droplets [24]. The ion mobility spectra of

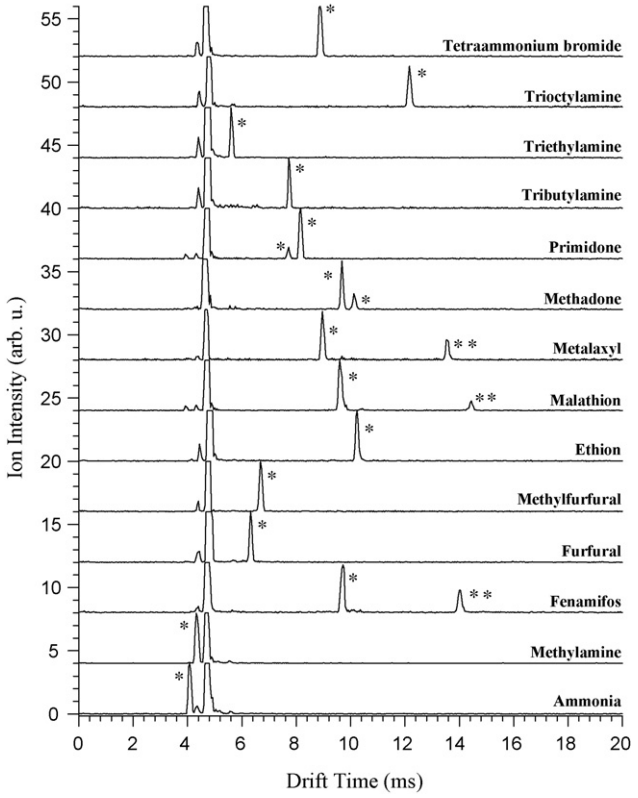

Fig. 2. The ion mobility spectra of the some compounds obtained at the optimum conditions of operating (Table 1). *Constituent ion peak of the compound. **Dimer ion formation.

various classes of compounds obtained in the optimized conditions are shown in Figs. 2 and 4.

Viidanoja et al. [30] suggested that tetraalkylammonium halides are ideal as mobility standards for ESI-IMS because these compounds generate only a single ion mobility peak in addition to their low tendency for clustering. In this work, tetrabutylammonium bromide was used as an external standard for the instrument. The absolute reduced mobility of this compound was calculated to be 1.26 $cm^2\ V^{-1}\ s^{-1}$, which is close to 1.33 $cm^2\ V^{-1}\ s^{-1}$, reported by Viidanoja et al. [30]. The K_0 value of this compound has not been reported using ^{63}Ni-IMS, presumably due to dissociation in the IMS cell. The reduced mobility values of all the compounds with unknown mobility were determined relative to this value according to Eq. (1).

$$\frac{K_0(\text{unknown})}{K_0(\text{standard})} = \frac{t_d(\text{standard})}{t_d(\text{unknown})} \quad (1)$$

In this equation, t_d is the drift time of the produced ion. The reduced mobility values of the produced ions for all the compounds studied in this work are listed in Table 2. In addition, the reduced mobility values of the compounds that are reported in the literatures using ^{63}Ni and electroapray are also tabulated in Table 2.

The reduced mobility values of some of these compounds such as furfural, methylfurfural, methadone and primidone are reported for the first time. As shown in Table 2, most K_0 values compared well with those obtained by ESI-IMS reports as well as with those obtained using ^{63}Ni-IMS. The exceptions were those of low molecular weight (ammonia and methylamine), which appeared in the region of the background solvent peaks. These compounds produce smaller ions than those of others under electrospray process. Based on the previous study conducted by Kebarle and Tang [31], solvation energy will increase when the size of the sprayed ion decreases. As a result, the desolvation process of the smaller ions produced by ammonia and methylamine can be more difficult than that of

Table 2
Reduced mobility values (K_o) and literature K_o values for several compounds employed in this study.

Compound	Class	Drift Time (ms), ±0.04	K_o ($cm^2\ V^{-1}\ s^{-1}$)	Lit. K_o ($cm^2\ V^{-1}\ s^{-1}$)	
				(ESI)	(^{63}Ni)[a]
Ammonia	Industrial	4.08	2.74	2.25 [28]	3.02 [24]
Methylamine	Industrial	4.32	2.59	2.21 [28]	2.65 [24]
Triethylamine	Industrial	5.84	1.92	1.84 [28]	1.95 [24]
Tributylamine	Industrial	7.94	1.41	1.35 [28]	1.38 [24]
Trioctylamine	Industrial	12.16	0.92		
Tetrabutylammonium bromide	Industrial	8.88	1.26	1.33 [30]	
Furfural	Industrial	6.32	1.77		
Methylfurfural	Industrial	6.68	1.67		
Ethion	Pesticide	10.24	1.09	1.06 [28]	1.20 [37]
Malathion	Pesticide	9.60	1.17	1.11 [28]	1.30 [37]
		14.44[b]	0.77	0.76 [28]	
Metalaxyl	Pesticide	9.08	1.23	1.15 [28]	1.37 [38]
		13.60[b]	0.82	0.77 [28]	
Fenamifos	Pesticide	9.72	1.15	1.08 [28]	
		14.04[b]	0.80	0.76 [28]	
Methadone	Drug	9.68	1.16		
		10.12	1.11		
Primidone	Drug	7.72	1.45		
		8.16	1.37		
Morphine	Drug	8.96	1.25	1.19 [28]	1.26 [33]
		9.32	1.20	1.15 [28]	1.22 [33]
Codeine	Drug	9.28	1.21	1.14 [28]	1.21 [33]
		9.56	1.17	1.10 [28]	1.18 [33]

[a] The reference values were obtained with air as the drift gas.
[b] The peak is might be due to the dimer ion formation.

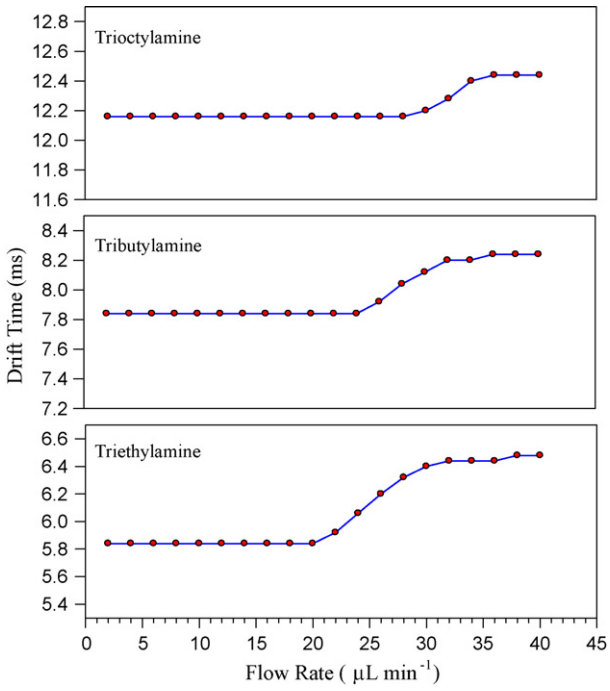

Fig. 3. The drift time of the peak of three compounds (triethyamine, tributylamine, and trioctylamine) was plotted versus flow rate of the sample solutions. The drift time values were constant at flow rates lower than 20, 22, and 30 μL min^{-1} for triethyamine, tributylamine, and trioctylamine, respectively.

larger ions. On the other hand, Hill et al. [24] have reported that the reduced mobility values for ammonia and methylamine determined by ESI-IMS are lower than those obtained by ^{63}Ni-IMS, and suggested that this is the consequence of inadequate desolvation of the analyte ions. Therefore, greater K_0 values obtained for ammonia and methylamine in this work with respect to those obtained through the previous instrument [28] might be due to more efficient desolvation of the compounds used in this work. Decreasing the volume of the desolvation chamber of the instrument to about half of the previous one increased the velocity of the drift gas exiting the drift chamber. This enhances the solvent evaporation of the electrosprayed droplets in the desolvation chamber. Although this geometry has been well known for the reaction region of the ^{63}Ni-IMS cell, it was investigated in ESI-IMS for the first time. In addition, in our old instrument, the desolvation gas was introduced to the cell in middle of the desolvation chamber, whereas in the new design, the gas enters the cell at the end of the desolvation region (near the shutter grid). This modification allows more effective solvent evaporation of the sprayed droplets by the desolvation gas. As Table 2 shows, the reduced mobility values reported in this study are much closer to those obtained by ^{63}Ni-IMS and therefore, it can be assumed that complete desolvation occurred by using proposed design for ESI-IMS.

To further survey the desolvation efficiency of the instrument, the individual IMS spectra of three amine compounds including triethyamine (TEA), tributylamine (TBA), and trioctylamine (TOA) at different flow rates were compared. The drift time of the peak of these compounds were plotted versus flow rate of the solution (Fig. 3). As this figure shows, the t_d values were constant at flow rates lower than 20, 22, and 30 μL min^{-1} for TEA, TBA, and TOA, respectively. At higher flow rates, the ion clusters possess more solvent molecules and the resulting large species are more difficult to desolvate, leading to slower mobility. Therefore, the ion cluster peaks shifted to a lower mobility and their drift time increased. Observation of different flow rates (20, 22, and 30 μL min^{-1}) might be due to different sizes of the sample molecules in the order of TEA < TBA < TOA. In summary, these results indicate that the complete solvent evaporation could be occurred even at fairly high flow rates, and consequently, would be helpful it to interface to HPLC columns.

Table 3
Comparison of resolving power obtained in this work with that of the previous instrument [28].

Compound	Resolving power, R_P	
	Proposed design	Previous instrument
Ethion	52.6 ± 0.4	41.0
Malathion	51.3 ± 0.8	40.7
Metalaxyl	68.4 ± 0.8	59.7
Tributhylamine	45.2 ± 0.5	34.5
Triethylamine	62.3 ± 0.6	
Furfural	70.4 ± 0.7	
Methy-furfural	61.8 ± 0.6	

3.2. Resolving power and resolution

In order to have an elementary understanding of the separation characteristics of the instrument, resolving power values for different compounds were measured and compared to the previously reported ones. Resolving power in IMS is defined as the drift time, t_d, of an ion divided by the peak width at half height, $w_{1/2}$ [22].

$$R_p = \frac{t_d}{w_{1/2}} \quad (2)$$

The measured resolving powers of the ion mobility spectrometer for some of the test compounds are summarized in Table 3. The resolving power for the studied compounds is quite striking and entirely typical of what was observed with this apparatus. As seen in Table 3, the resolving power values obtained in this work are increased by about 15–30% compared to those obtained with our old instrument [28].

As described in the previous section, this new design speeds up the solvent evaporation process in the desolvation region before the ions are injected into the drift region. This enhances the evaporation of further solvent molecules from the clusters to produce ion clusters with the lower numbers of solvent molecules, producing a narrower peak and consequently a higher resolving power. The resolving power values obtained in this work can be compared with the range of 65–95, reported by Collins and Lee [32], where they used a 27 cm drift tube length and a 200 μs pulse width.

In order to find out the effect of each modification (smaller diameter of the desolvation region and positioning of the desolvation gas) on desolvation efficiency, it is required to do more experiments. In this regard, the resolving power of the ethion and malathion were re-calculated by instrument without the modification of desolvation gas position. The resolving power of ethion and malathion were obtained 49.8 and 49.1, respectively. These data show about 21% increase in resolving power values with respect to our old instrument, and consequently, it seems that the factor of decreasing the diameter of desolvation rings has more effect on improvement of the resolving power of the instrument.

To further investigate the power of the instrument for practical separation of the closely spaced peaks, ion mobility spectra of morphine and codeine were obtained and compared with those obtained previously [28] (Fig. 4). According to Fig. 4, these drugs produce two adjacent ion peaks, M_1 and M_2 for morphine and C_1 and C_2 for codeine.

According to Table 2, the ion clusters are comparable with those obtained by Lawrence [33]. This figure clearly indicates that, in the new instrument, the two peaks are completely baseline resolved for

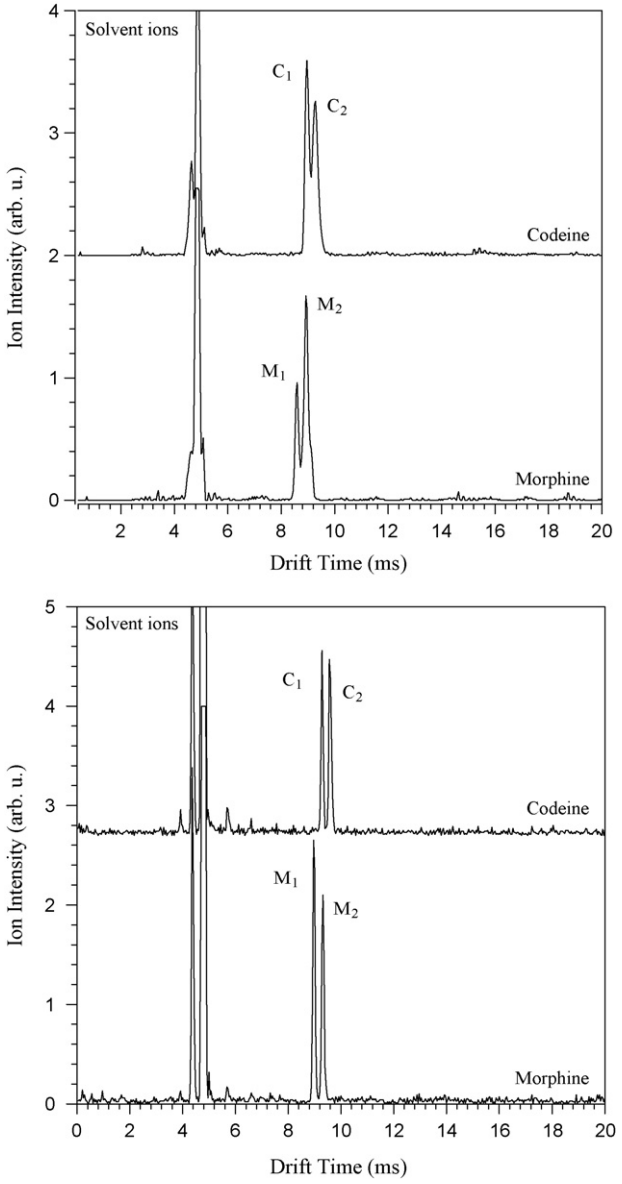

Fig. 4. Comparison of the ion mobility spectra of morphine and codeine obtained in this work (bottom) with those obtained by previous instrument [28] (top). It is clearly indicated that in the new instrument the two peaks are completely baseline resolved for each drug compound.

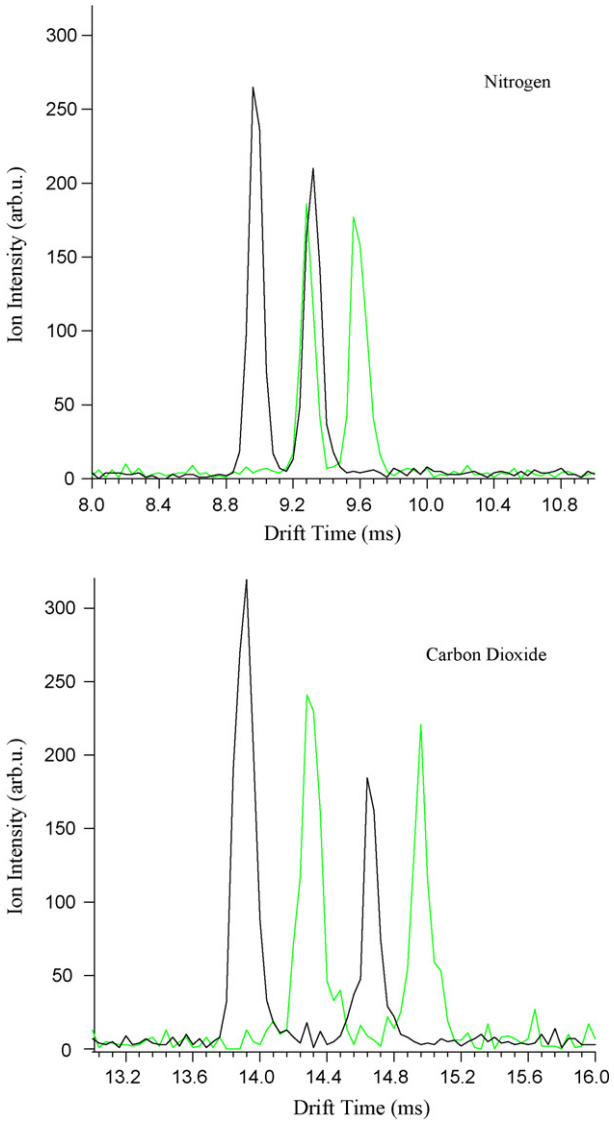

Fig. 5. Overplot of ion mobility spectra of morphine and codeine with N_2 and CO_2 as drift gases. The spectra demonstrate that the use of CO_2 can separate two peaks of morphine from those of the codeine.

each drug compound, while this was not the case for the old apparatus. The peak-to-peak resolution, R_{pp}, was calculated for morphine and codeine ion clusters, based on Eq. (3).

$$R_{pp} = \frac{2\Delta t_d}{w_{b1} + w_{b2}} \quad (3)$$

where Δt_d is the difference between drift times of the two adjacent peaks and the w_{b1} and w_{b2}, are their corresponding peak widths. The resolution values were 1.5 and 1.3 for morphine and codeine compounds, respectively. However, the drift time of the M_2 (9.32 ms) and C_1 (9.28 ms) are the same and therefore, each drug interferes with the other one in the analysis of real samples. Since the analysis of these two compounds is very important in biological matrices, full separation of their IMS signals was attempted in this work. Changing the drift gas can drastically improve the separability in ion mobility spectrometry [15,34]. Therefore, the ion mobility spectra of morphine and codeine using nitrogen or carbon dioxide as the drift gas were obtained (Fig. 5). According to Fig. 5, M_2 and C_1 peaks were indistinguishable in nitrogen while they were easily separated in carbon dioxide. In this work, two adjusted ion peaks of morphine (M_1 and M_2) were completely separated from those of codeine (C_1 and C_2) for the first time. Consequently, it can be possible to determine these drugs in presence of each other.

3.3. Electrospray ionization efficiency

As described in Section 3.1, complete desolvation can be obtained with present instrument at higher flow rates than that of the previous instrument. It was expected that the intensity of the IMS signal would increase at higher flow rates. But different results were observed, especially at high analyte concentrations. In this regard, we thoroughly investigated the variation of the peak intensity at a wide range of flow rate (from 1 to 40 $\mu L\,min^{-1}$). Fig. 6 shows plots of peak intensities extracted from IMS spectra for different concentrations of tributylamine as a function of flow rate.

These plots show three regions including an uphill, plateau, and downhill for all concentrations. When the plots start to plateau, it

Table 4
Analytical parameters for ethion, metalaxyl, and tributylamine using ESI–IMS.

Parameter	Ethion	Metalaxyl	Tributylamine
Calibration curve formula	$Y = 0.01 + 5.63X$	$Y = 0.09 + 2.98X$	$Y = 0.04 + 9.02X$
Linear Range ($\mu g\,mL^{-1}$)	0.05–2.20	0.10–1.80	0.02–1.20
Correlation Coefficient, R^2	0.9986	0.9968	0.9970
Detection Limit ($\mu g\,L^{-1}$)	16	38	6
Relative Standard Deviation, RSD (%) for 0.4 $\mu g\,mL^{-1}$ and $n = 5$	6.4	8.1	7.3

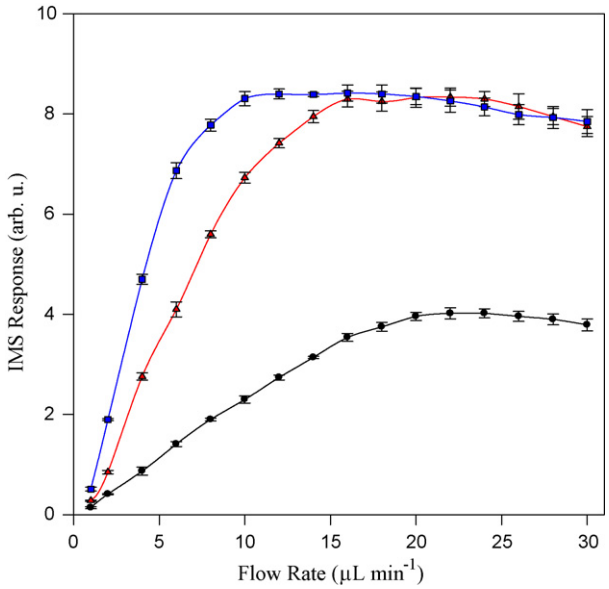

Fig. 6. Plots of IMS response versus flow rate for tributylamine at different concentrations of 0.1 (●), 0.5 (▲), and 1.0 $\mu g\,mL^{-1}$ (■) included three regions of uphill, plateau, and downhill.

indicates that the total number of ions detected at the Faraday plate has reached maximum and when the plots start to decline, it is clear that total ions produced by electrospray process have decreased. Fig. 6 also shows that when the sample concentration increases, the plateau and downhill regions are shifted to lower flow rates. To interpret these results, we considered the number of ions detected by the Faraday plate (n), as derived by Hill and co-workers [35]:

$$n = n'\mathrm{DE\%} = cft_g N_{avg}\mathrm{DE\%} \quad (4)$$

where n' is the total number of analyte molecules introduced to electrospray region and DE% is the detection efficiency percentage. n is dependent on the concentration of analyte (c, in molar), flow rate (f, in $L\,s^{-1}$), and shutter grid pulse (t_g, in second). N_{avg} is the Avogadro's number. On the other hand, according to Hill's report [35], the detection efficiency (DE%) is dependent on ionization efficiency (IE%) and ion transmission (TE%) as:

$$\mathrm{DE\%} = \mathrm{IE\%} \times \mathrm{TE\%} \quad (5)$$

The ion transmission (TE%) can be assumed 100% in ESI-IMS due to the large entrance so that it is possible to receive total ion plume produced by the electrospray. In addition, it is clear that in the electrospray process, the ionization efficiency (IE%) increased when the flow rate decreased [35]. Increasing the flow rate at low region, increases the number of ions detected (n), resulting in enhanced peak intensity. In this case n' is a dominant term in Eq. (4) and the plots in Fig. 6 are in uphill region. At the plateau region, when the flow rate further increases, n also increases while the ionization efficiency further decreases, and therefore, the peak intensity remains approximately constant. If the flow rate further increases after plateau region, ionization efficiency becomes the dominating factor and ion response will eventually decrease.

3.4. Analytical parameters

In this work, a series of standards in the range 0.01–20 $\mu g\,mL^{-1}$ of ethion, metalaxyl, and tributylamine were prepared in methanol and used to determine the analytical parameters of the instrument. When a stable electrospray was achieved, the area of the ion peak produced from IMS system was calculated and considered as the response of ESI-IMS for each concentration of the individual compounds. Ten ion mobility spectra were acquired to obtain the averaged data points. The areas under ion peak(s) were plotted against concentration of these compounds and calibration curve equations were developed by least-squares method. The analytical parameters of the proposed ESI-IMS method for the determination of these compounds are summarized in Table 4.

As this table shows, the linearity range for ethion, metalaxyl, and tributylamine is 0.05–2.20, 0.10–1.80, and 0.02–1.20 $\mu g\,mL^{-1}$, respectively. The data show the linear dynamic range of about 2 orders of magnitude, which is typical for ESI sources and for most IMS systems [36]. Using the standard definition of S/N = 3, the detection limits of 16, 38, and 6 $\mu g\,L^{-1}$ were determined for ethion, metalaxyl, and tributylamine, respectively. The detection limits obtained in this work are in the range 10–1340 $\mu g\,L^{-1}$, as reported by Asbury et al. for various compounds [36]. The correlation coefficients were greater than 0.99 for all the compounds. These results compare favorably to the other techniques such as ^{63}Ni-IMS [37,38]. The quantitative results obtained in this work are promising for further development of this method as an analytical tool for the detection of various compounds in liquid samples.

4. Conclusions

An improved design for ESI-IMS cell was introduced and its performance was investigated. In this design, the diameter of desolvation region was decreased and the desolvation gas entered the cell at the end of this region. The consequence of these changes was to increase the desolvation efficiency at higher flow rates and therefore, the resolving power or resolution of the apparatus was enhanced. A resolving power of about 70 could be achieved by only 11 cm drift tube length and 300 μs pulse width. It was shown that the baseline separation of two adjacent ion peaks of morphine and codeine could be achieved with resolutions of 1.5 and 1.3, respectively. In this work, thorough investigation of the drift time as well as the IMS signal for ion clusters was studied at a wide range of the sample flow rates. Additionally, the electrospray ionization occurred outside the cell oven, enabling us to use the instrument without needle clogging and disturbance of the electrospray process even at a temperature as high as 200 °C. Finally, the calibration curves for determination of ethion, metalaxyl, and tributylamine were obtained, and the analytical parameters revealed capability of the instrument for quantitative analysis.

Acknowledgements

The author is very grateful to the Research Council of Isfahan University of Technology for financial support of this work. Dr. Rezaei and Dr. Khayamian are also specially acknowledged for their valuable helping and discussions. Sincerely thank to Prof. Amini (Isfahan University) and Prof. Amirnasr for their review of the text.

References

[1] G.A. Eiceman, Z. Karpas, Ion Mobility Spectrometry, 2nd ed., CRC Press, Boca Raton, FL, 2005.
[2] S.J. Valentine, M.D. Plasencia, X. Liu, M. Krishnan, S. Naylor, H.R. Udseth, R.D. Smith, D.E. Clemmer, J. Proteome Res. 5 (2006) 2977.
[3] J.A. Taraszka, X. Gao, S.J. Valentine, R.A. Sowell, S.L. Koeniger, D.F. Miller, T.C. Kaufman, D.E. Clemmer, J. Proteome Res. 4 (2005) 1238.
[4] S. Myung, J.M. Wiseman, S.J. Valentine, T. Zoltán, R.G. Cooks, D.E. Clemmer, J. Phys. Chem. B 110 (2006) 5045.
[5] F.W. Karasek, Res. Dev. 21 (1970) 34.
[6] F.W. Karasek, W.D. Kilpatrick, M.J. Cohen, Anal. Chem. 43 (1971) 1441.
[7] C.S. Hoaglund, S.J. Valentine, C.R. Sporleder, J.P. Reilly, D.E. Clemmer, Anal. Chem. 70 (1998) 2236.
[8] D.E. Clemmer, M.F. Jarrold, J. Mass Spectrom. 32 (1997) 577.
[9] L.W. Beegle, I. Kanik, L. Matz, H.H. Hill, Anal. Chem. 73 (2001) 3028.
[10] H.M. Dion, L.K. Ackerman, H.H. Hill, Talanta 57 (2002) 1161.
[11] A.B. Kanu, H.H. Hill, Talanta 73 (2007) 692.
[12] A.B. Kanu, H.H. Hill, J. Chromatogr. A 1177 (2008) 12.
[13] D.G. McMinn, J.A. Kinzer, C.B. Shumate, W.F. Siems, H.H. Hill, J. Microcol. Sep. 2 (1990) 188.
[14] Y.H. Chen, H.H. Hill, D.P. Wittmer, J. Microcol. Sep. 6 (1994) 515.
[15] G.R. Asbury, H.H. Hill, J. Microcol. Sep. 12 (2000) 172.
[16] L.M. Matz, H.M. Dion, H.H. Hill, J. Chromatogr. A 946 (2002) 59.
[17] R.W. Hallen, C.B. Shumate, W.F. Siems, T. Tsuda, H.H. Hill, J. Chromatogr. 480 (1989) 233.
[18] M. McCooeye, L. Ding, G.J. Gardner, C.A. Fraser, J. Lam, R.E. Sturgeon, Z. Mester, Anal. Chem. 75 (2003) 2538.
[19] C.B. Shumate, H.H. Hill, Anal. Chem. 61 (1989) 601.
[20] C. Shumate, Trends Anal. Chem. 13 (1994) 104.
[21] M. Tam, H.H. Hill, Anal. Chem. 76 (2004) 2741.
[22] W.F. Siems, C. Wu, E.E. Tarver, H.H. Hill, P.R. Larsen, D.G. McMinn, Anal. Chem. 66 (1994) 4195.
[23] M.L. Gieniec, J. Cox Jr., D. Teer, M. Dole, 20th Annual Conference on Mass Spectrometry and Allied Topics, Dallas, TX, June 4–9, 1972.
[24] D. Wittmer, Y.H. Chen, B.K. Luckenbill, H.H. Hill, Anal. Chem. 66 (1994) 2348.
[25] G.R. Asbury, H.H. Hill, Int. J. Ion Mobility Spectrom. 2 (1999) 1–8.
[26] Y.H. Chen, H.H. Hill Jr., D.P. Wittmer, Int. J. Mass Spectrom. Ion Proc. 154 (1996) 1.
[27] D.S. Lee, C. Wu, H.H. Hill Jr., J. Chromatogr. A 822 (1998) 1.
[28] T. Khayamian, M.T. Jafari, Anal. Chem. 79 (2007) 3199.
[29] N.E. Bradbury, R.A. Nielsen, Phys. Rev. 49 (1936) 388.
[30] J. Viidanoja, A. Sysoev, A. Adamov, T. Kotiaho, Rapid Commun. Mass Spectrom. 19 (2005) 3051.
[31] P. Kebarle, L. Tang, Anal. Chem. 65 (1993), 972 A.
[32] D.C. Collins, M.L. Lee, Fresenius J. Anal. Chem. 369 (2001) 225.
[33] A.H. Lawrence, Anal. Chem. 58 (1986) 1269.
[34] L.M. Matz, H.H. Hill, L.W. Beegle, I. Kanik, J. Am. Soc. Mass Spectrom. 13 (2002) 300.
[35] X. Tang, J.E. Bruce, H.H. Hill, Anal. Chem. 78 (2006) 7751.
[36] G.R. Asbury, C. Wu, W.F. Siems, H.H. Hill, Anal. Chim. Acta 404 (2000) 273.
[37] M.T. Jafari, Talanta 69 (2006) 1054.
[38] M.T. Jafari, M. Azimi, Anal. Lett. 39 (2006) 2061.